

# Influence of Incidence Angle on the Electrical Parameters of a vertical Silicon Solar Cell under Frequency Modulation

Moustapha SANE, Martial ZOUNGRANA, Hawa LY DIALLO, Gokhan SAHIN, Ndeye THIAM, Mor NDIAYE, MOUSTAPHA DIENG, Grégoire SISSOKO

**Abstract:** A theoretical study of a vertical junction silicon solar cell in frequency modulation, with incidence angle effect under a monochromatic illumination has been done. Based on the diffusion-recombination equation, the expression of excess minority carrier density in the base was established according to the modulation frequency and the illumination incidence angle. Photocurrent density, photovoltage, series and shunt resistances are then deduced. The objective of this work is to show the effects of both modulation frequency and illumination incidence angle on these electrical parameters.

**Keywords:** Vertical junction - incidence Angle - frequency modulation.

## I. INTRODUCTION

Solar cells performance is quite limited by recombination processes (Orton et al., 1990); it is then of great importance to identify and limit the effects of these recombination through the knowledge of certain parameters and the control of the associated technological processes.

Many methods have then been developed for solar cells characterization in steady state (Sze et al., 2007), quasi-steady state (Diallo et al., 2008; Mbojji et al., 2011), transient state (Barro F. I. et al., 2010; Gueye I et al., 2012) and frequency modulation (Dieng et al., 2011; A. Thiam, et al., 2012).

In this work, we will first determine the excess minority carrier density, the photocurrent and the voltage across the junction. Based on the I-V curve, the series and shunt resistances are then calculated. The aim of this study is to show the effects of both modulation frequency and illumination incidence angle on the solar cell.

**Manuscript received October, 2013.**

**Moustapha SANE**, Laboratory of Semiconductors and Solar Energy, Physics Department, Faculty of Science and Technology, University Cheikh Anta Diop, Dakar, Senegal

**Martial ZOUNGRANA**, Laboratory of Materials and Environment, UFR/SEA, University of Ouagadougou, Burkina Faso

**Hawa LY DIALLO**, 3University of Thies, UFR SET, University of Thies, Senegal

**Gokhan SAHIN**, Laboratory of Semiconductors and Solar Energy, Physics Department, Faculty of Science and Technology, University Cheikh Anta Diop, Dakar, Senegal

**Ndeye THIAM**, Laboratory of Semiconductors and Solar Energy, Physics Department, Faculty of Science and Technology, University Cheikh Anta Diop, Dakar, Senegal

**Mor NDIAYE**, Laboratory of Semiconductors and Solar Energy, Physics Department, Faculty of Science and Technology, University Cheikh Anta Diop, Dakar, Senegal

**MOUSTAPHA DIENG**, Laboratory of Semiconductors and Solar Energy, Physics Department, Faculty of Science and Technology, University Cheikh Anta Diop, Dakar, Senegal

**Grégoire SISSOKO**, Laboratory of Semiconductors and Solar Energy, Physics Department, Faculty of Science and Technology, University Cheikh Anta Diop, Dakar, Senegal

For that purpose, excess minority carrier density, photocurrent, photovoltage, series and shunt resistances are studied for various incidence angles in frequency modulation.

## II. THEORY

This study is based on a vertical parallel junction solar cell presented on figure 1.

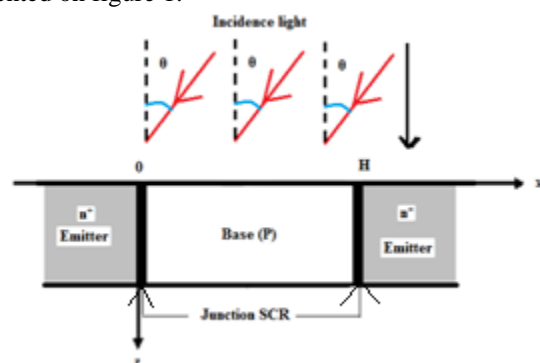


**Fig. 1: Vertical parallel junction silicon solar cell**

Given that the contribution of the base to the photocurrent is larger than that of the emitter (Barro et al., 2001; Lemrabott et al., 2008), our analysis will only be developed in the base region. We also consider a Quasi-Neutral Base (Q.N.B) neglecting the electrical field within the base of the solar cell.

The distribution of the minority carrier's photogenerated (electrons) in the base is governed by the diffusion-recombination equation.

Taking into account the generation, recombination and diffusion phenomena in the base, the equation, governing the variation of the excess minority carriers in frequency modulation (Honma et al., 1987; Thiam Nd et al., 2012 ) can be written as:

$$D(\omega) \cdot \frac{\partial^2 \delta(x, \theta, t)}{\partial x^2} - \frac{\delta(x, \theta, t)}{\tau} = -G(z, \theta, t) + \frac{\partial \delta(x, \theta, t)}{\partial t} \quad (1)$$

$$\text{where } \delta(x, t) = \delta(x) \exp(-j\omega t) \quad (2)$$

$$\text{and } G(z, \theta, t) = g(z, \theta) \exp(-j\omega t) \quad (3)$$

with

$$g(z, \theta) = \alpha_i (1 - R_i) \cdot \phi_i \cdot \exp(-\alpha_i \cdot z) \cdot \cos(\theta) \quad (4)$$

x is the base depth on x axis,  $\omega$  is the modulation frequency,  $\theta$  is the incidence angle, z is the base depth along z axis, Sf is the junction recombination velocity and  $\lambda$  is the illumination wavelength.

Inserting (4) into (3), (3) into (2) and replacing  $\delta(x)$  into (1) by equation (2) the time dependent part of equation (1) is eliminated and we obtain:

$$\frac{\partial^2 \delta(x)}{\partial x^2} - \frac{\delta(x)}{L(\omega)^2} = -\frac{g(x, \theta)}{D(\omega)} \quad (5)$$

The solution of this equation is:

$$\delta(x, \omega, \theta, z, Sf, \lambda) = A \cosh\left(\frac{x}{L(\omega)}\right) + B \sinh\left(\frac{x}{L(\omega)}\right) +$$

$$\frac{L(\omega)^2}{D(\omega)} \cdot \alpha_r (1 - R_r) \cdot \phi_r \cdot \exp(\alpha_r \cdot z) \cdot \cos(\theta) \quad (6)$$

Coefficients A and B are determined based on the following boundary conditions:

- At  $x = 0$ , (junction)

$$D(\omega) \cdot \left. \frac{\partial \delta(x, \omega, \theta)}{\partial x} \right|_{x=0} = Sf \cdot \delta(x, \omega, \theta) \Big|_{x=0} \quad (7)$$

- At  $x = H/2$ , (middle of the base)

$$D(\omega) \cdot \left. \frac{\partial \delta(x, \omega, \theta)}{\partial x} \right|_{x=\frac{H}{2}} = 0 \quad (8)$$

### III. RESULTS AND DISCUSSION

Figure 2 presents the profile of the excess minority carrier density versus base depth along x axis for various incidence angles.

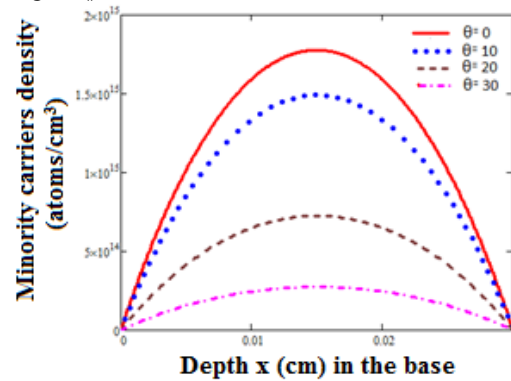


**Fig. 2: Excess minority carrier density versus base depth x for various incidence angles.  $\omega = 105 \text{ rad/s}$ ,  $Sf = 4.104 \text{ cm/s}$ ,  $H = 0.03 \text{ cm}$ ,  $L_0 = 0.0001 \text{ cm}$ ,  $D_0 = 26 \text{ cm}^2/\text{s}$ ,  $\tau = 10^{-5} \text{ s}$ ,  $z = 0.0001 \text{ cm}$ ,  $\lambda = 0.5 \mu\text{m}$ .**

This figure shows that excess minority carriers density increase below a certain depth in the base and above that depth it decrease with base depth. That is, given the presence of the two junctions at both sides of the base, photogenerated carriers in the base flow in to two directions: the two junctions. These flows of carriers through the two junctions lead to a decrease of the excess minority carriers when moving to the junction.

Thanks to the presence of the two junctions, the photocurrent obtained is more important than that of a single junction. This is undoubtedly an advantage of vertical parallel junction solar cells.

We can also observe a decrease of the excess minority carrier density for the chosen incidence angles as observed with the other parameters.

Photocurrent: The photocurrent density is given by the following expression:

$$J_{ph} = 2 \cdot q \cdot D(\omega) \cdot \left. \frac{\partial \delta(x, \omega, \theta)}{\partial x} \right|_{x=0} \quad (9)$$

A plot of the photocurrent density versus modulation frequency for various incidence angles is presented on

figure 3 below.

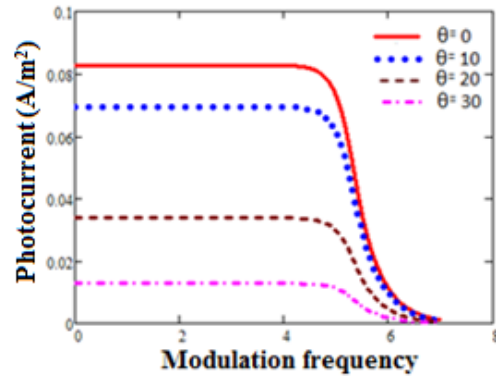


**Fig. 3: Photocurrent density versus modulation frequency (log scale) for various incidence angles.  $Sf = 4.104 \text{ cm/s}$ ,  $H = 0.03 \text{ cm}$ ,  $L_0 = 0.0001 \text{ cm}$ ,  $D_0 = 26 \text{ cm}^2/\text{s}$ ,  $\tau = 10^{-5} \text{ s}$ ,  $z = 0.0001 \text{ cm}$ ,  $\lambda = 0.5 \mu\text{m}$**

This plot shows that photocurrent density doesn't depend significantly on the modulation below a certain modulation frequency  $\omega c$ ; above that threshold, the photocurrent density decreases very markedly and rapidly like in a low pass filter. Effectively for higher modulation frequencies carrier cannot relaxate quickly so that they cannot diffuse to the junction. The collected carriers will decrease leading to a decrease of the photocurrent.

We also note that the photocurrent decrease with increasing incidence angle. Really, the dependence of the photocurrent on the incidence angle is expressed by a cosine law as presented early by (Balenzategui et al., 2005).

We now present on figure 4, the profile of the photocurrent versus junction recombination velocity for various angles of incidence.

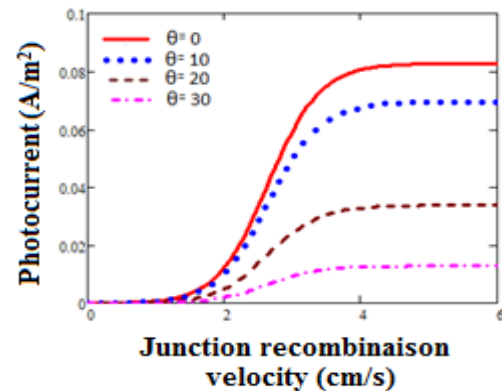


**Fig. 4: Photocurrent density versus junction recombination velocity for various incidence angles.  $\omega = 105 \text{ rad/s}$ ,  $H = 0.03 \text{ cm}$ ,  $L_0 = 0.0001 \text{ cm}$ ,  $D_0 = 26 \text{ cm}^2/\text{s}$ ,  $z = 0.0001 \text{ cm}$ ,  $\tau = 10^{-5} \text{ s}$ ,  $\lambda = 0.5 \mu\text{m}$ .**

Figure 4 shows that the photocurrent increase with the junction recombination velocity; effectively, if we keep in mind that junction recombination velocity  $Sf$  traduces the flow of carriers through the junction (Diallo et al., 2008; Diallo et al., 2012), we can say that for low  $Sf$ , there is a very low carrier flow through the junction leading to lower photocurrent generated, as observed. Generated carriers are stored on both sides of the junction and the solar cell operates near open-circuit.

For higher  $Sf$ , the carrier flow through the junction increases so that the generated photocurrent also increases: the solar cell operates near short circuit.

Photovoltage: According to the Boltzmann relation, the photovoltage is obtained by the expression (10).

$$V = V_T \cdot \ln \left[ 1 + \frac{Nb}{n_0^2} \cdot \delta(0) \right] \quad (10)$$

with

$$V_T = \frac{K \cdot T}{q} \quad (11)$$

Nb is the base doping density; n0 is the intrinsic carrier's density thermal equilibrium; K is the Boltzmann constant; T is the absolute temperature and q is the elementary charge. The photovoltage profile for various values of the incidence angle is given on figure 5.

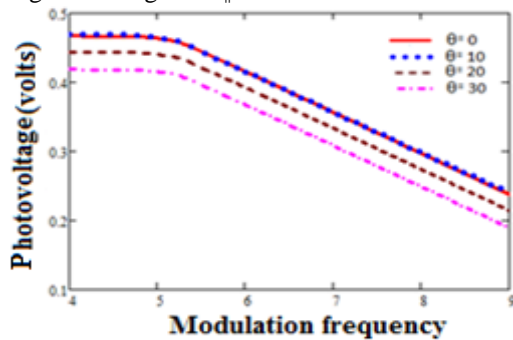


**Fig. 5: Photovoltage versus modulation frequency (log scale) for various incidence angles. Sf = 4.104cm/s, H=0.03cm , Lo=0.0001cm , Do=26cm<sup>2</sup>/s, τ=10-5s, z = 0.0001cm, λ=0.5μm**

The photovoltage decreases with increasing modulation frequency but this decrease is more marked above a certain threshold as for photocurrent density.

For higher modulation frequencies, carriers cannot diffuse and are recombined in the base so that there is no carrier collection no carrier storage across the junction.

Figure 6 presents the profile of the photovoltage versus junction recombination velocity for various incidence angles.

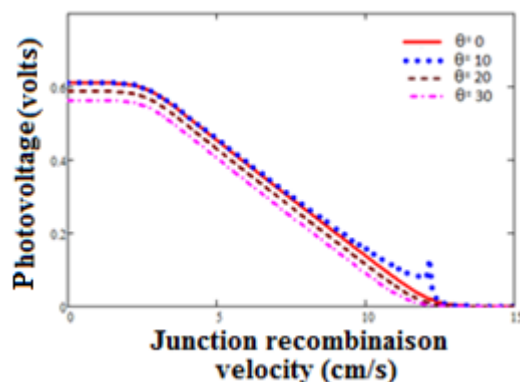


**Fig. 6: Photovoltage incidence angles. ω=105rad/s, H=0.03cm, Lo=0.0001cm, Do=26cm<sup>2</sup>/s, τ=10-5s, z = 0.0001cm, λ=0.5μm.versus junction recombination velocity for various**

For lower junction recombination velocities, carriers flow through the junction is neglectable since carriers are stored across the junction: the photovoltage is at the maximum value (open-circuit voltage).

For increasing Sf value, carriers flow through the junction increase and the stored charge cross the junction leading to a decrease of the photovoltage.

Shunt and series resistances: The determination of shunt and series resistances is based on the behavior of the solar cell I-V curve respectively near short-circuit and open-circuit. It

has been proved (Mbodji et al., 2012) that near short-circuit, the solar cell behaves like a real current generator; that is, there is a parasitic resistance in parallel with an ideal current generator. This parasitic resistance is the shunt resistance Rsh. Shunt resistance characterizes junction quality: higher Rsh value means good junction properties with minimum current lost and low Rsh value means maximum current lost essentially by interface states in the junction and short-circuit at junction boundaries (Kunz et al., 2008).

Near open-circuit, solar cell behaves like a real voltage generator with a parasitic resistance in series with an ideal voltage generator (Mbodji et al., 2012), this parasitic resistance is the series resistance Rs (Wenham et al., 2007). Rs characterizes quasi-neutral region resistances, semiconductor-metal contact resistance and metal grid contact resistance (Wenham et al., 2007).

Based on a previous work (Mbodji et al., 2012), the equations giving shunt and series resistances are expressed as:

$$R_s(Sf) = \frac{V_{co} - V_{ph}(Sf)}{J_{ph}(Sf)} \quad (12)$$

Very low Sf value

$$R_{sh}(Sf) = \frac{V_{ph}(Sf)}{J_{cc} - J_{ph}(Sf)} \quad (13)$$

Very high Sf value

In these equations, Voc is the open-circuit voltage, Jsc is the short-circuit current density.

Figure 7 presents the profile of the series resistance versus junction recombination velocity for various angles of incidence.

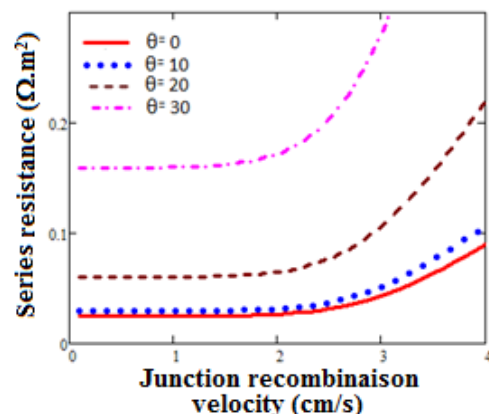


**Fig. 7: Series resistance versus junction recombination velocity for various incidence angles. ω=105rad/s, H=0.03cm, Lo=0.0001cm, Do=26cm<sup>2</sup>/s, τ=10-5s, z = 0.0001cm, λ=0.5μm.**

Figure 7 shows that series resistance increase with junction recombination velocity; effectively, when junction recombination velocity increase, there is more and more carriers living the base region and crossing the junction so that free carriers density directly decreases. This decrease leads to an increase of the base dynamic mobility and thus its resistivity; that is why series resistance increases with junction recombination velocity.

Figure 7 also shows that series resistance increases with incidence angle.

The profile of shunt resistance versus junction recombination velocity is presented on figure 8.

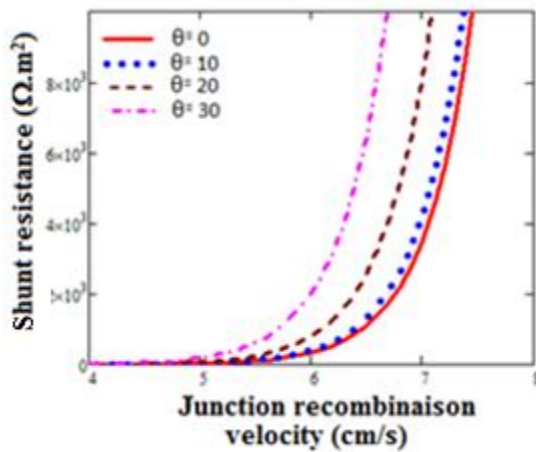


**Fig. 8: Shunt resistance versus junction recombination velocity for various angles of incidence of the light.**  
 $\omega=105\text{rad/s}$ ,  $H=0.03\text{cm}$ ,  $L_0=0.0001\text{cm}$ ,  $D_0=26\text{cm}^2/\text{s}$ ,  
 $\tau=10\text{-}5\text{s}$ ,  $z = 0.0001\text{cm}$ ,  $\lambda=0.5\mu\text{m}$ .

One can see that shunt resistance also increase with both junction recombination velocity and incidence angle but the influence of incidence angle is more marked for very high Sf values.

Increasing of shunt resistance with junction recombination velocity is mainly governed by the fact that solar cell dynamic resistivity increase when junction recombination increase, as for series resistance.

#### IV. CONCLUSION

A theoretical study of a vertical junction solar cell has been presented. Electrical parameters such as photocurrent density, photovoltage, series and shunt resistances have been determined and we showed the effects of modulation frequency and illumination incidence angle. This study exhibit the fact that photocurrent density and photovoltage do not depend on modulation frequency below a certain threshold which is the quasi steady state limit. Above that threshold, both photocurrent density and photovoltage decrease rapidly.

It has also been shown that all the studied parameters depend on illumination incidence angle by a cosine law. Solar panels must then be installed on sit taking into account both the site's latitude and the cosine law to optimize the performance of the solar panels.

#### REFERENCES

1. Ahmed, F., and S. Garg. 1986. International centre for theoretical physics, Trieste, Italy Internal Report. Thiam, M. Zougrana, H. Ly Diallo, A Diaio,
2. N. Thiam, . S. Gueye, M.M. Deme, M. Sarr and G. Sissoko,
3. Influence of Incident Illumination Angle on Capacitance of a Silicon Solar Cell under Frequency Modulation, Research Journal of Applied Sciences, Engineering and Technology 5(4), pp 1123-1128, (2013).
4. Balenzategui, J.L., F. Chenlo, 2005. Measurement and analysis of angular response of bare and encapsulated silicon solar cells Solar Energy Materials & Solar Cells 86 53–83
5. Barro, F. I., A S Maiga, Wereme A, Sissoko G 2010. Determination of recombination parameters in the base of a bifacial silicon solar cell under constant multispectral light ; Phys. Chem. News 56 76-84
6. Bousse, L., S. Mostarshed, D. Hafeman, M. Sartore, M. Adami et C. Nicolini. 1994. Investigation of carrier transport through silicon wafers by photocurrent measurements. J. Appl. Phys. Vol.75 (8): 4000 – 4008.
7. Diallo, H. L., A. S. Maïga, A. Werene, G. Sissoko. 2008. “New approach of both junction and back surface recombination velocities in a 3D modeling study of a polycrystalline silicon solar cell”, Eur.Phys.J.Applied.phys.42, 203-211.
8. Diallo. H. Ly., B. Dieng, I. Ly, M.M. Dione, M. Ndiaye, O.H.

- Lembrabott, Z.N. Bako, A. Wereme and G. Sissoko, 2012. Determination of the Recombination and Electrical Parameters of a Vertical Multijunction Silicon Solar Cell. Res.J. Appl. Sci. Engineering Technol. Maxwell scientific Organization, 3(7): 602-611, ISSN: 2040-7467.
9. Dieng A., I. Zerbo, M. Wade, A. S. Maiga and G. Sissoko, 2011. Three-dimensional study of a polycrystalline silicon solar cell: the influence of the applied magnetic field on the electrical parameters, Semicond. Sci. Technol. 26 095023 (9pp).
10. Dieng, A., N. Thiam, A. Thiam, A.S. Maiga and G.Sissoko, 2011, Magnetic field effect on the electrical parameters of a polycrystalline silicon solar cell. Res.J. Appl. Sci. Eng. Techn., 3(7): 602-611.
11. Honma N and Munakata C, 1987. Sample thickness dependence of minority carrier lifetimes measured using an ac photovoltaic method Japan. J. Appl. Phys. 26 2033–6
12. Kunz, O., J. Wong, J. Janssens, J. Bauer, O. Breitenstein and A.G. Aberle, 2008. Shunting Problems Due to Sub-Micron Pinholes in Evaporated Solid-Phase Crystallised Poly-Si Thin-Film Solar Cells on Glass. Prog. Photovolt: Res. Appl. 2009; 17:35–46
13. Mbodji S., B. Mbow, F. I. Barro and G. Sissoko, 2011. A 3D model for thickness diffusion capacitance of emitter-base junction determination in a bifacial polycrystalline solar cell under real operating condition; Turk J Phys 35 281-291
14. Mbodji, S., I. Ly, H.L. Diallo, M.M. Dione, O. Diasse and G. Sissoko, 2012. Modeling study of n+/p solar cell resistances from single I-V characteristic curve considering the junction recombination velocity (Sf). Res. J. Appl. Sci. Eng. Techn., 4(1): 1-7.
15. Misiakos, K., C. H. Wang, A. Neugroschel, and F. A. Lindholm, 1990. Simultaneous Extraction of minority-carrier parameters in crystalline semiconductors by lateral photocurrent, J. Appl. Phys. 67 (1): 321 – 333.
16. Mohammad, S.N., 1987. An alternative method for the performance analysis of silicon solar cells, J. Appl. Phys. 61 (2): 767 – 772.
17. Thiam Nd., A. Diaio, M. Ndiaye, A. Dieng, A. Thiam, M. Sarr, A.S. Maiga and G. Sissoko, 2012. Electric equivalent models of intrinsic recombination velocities of a bifacial silicon solar cell under frequency modulation and magnetic field effect. Res.J. Appl. Sci. Engineering Technol. Maxwell Scientific Organization, 3(7): 602-611.
18. Orton, J.W. and P. Blood, 1990. The Electrical Charactization of Semiconductor: Measurement of Minority Carrier Properties. Academic Press, London.
19. Sissoko, G., C. Museruka, A. Corréa, I. Gaye, A. L. Ndiaye, 1996. World Renewable Energy Congress. part III, pp.1487-1490
20. Sze S M and Kwok K Ng, 2007. Physics of Semiconductors Devices (New York: Wiley)
21. Wenham, S. R., M. A. Green, M. E. Watt, R. Corkish, 2007. Applied Photovoltaics, Second Edition. Copyright © 2007, ARC Centre for Advanced Silicon Photovoltaics and Photonics.
22. Wise, J.F., 1970. Vertical junction solar cell. U.S Patent 3690953,
23. Zougrana. A. M., N. Thiam, S. Gueye, M. M .Deme, M. Sarr and G. Sissoko, 2012. Influence of Incident Illumination Angle on Capacitance of a Silicon Solar Cell Under Frequency Modulation; Research Journal of Applied Sciences, Engineering and Technology; Maxwell Scientific Organization.